AJNR

Effects of Agmatine on Blood-Brain Barrier Stabilization Assessed by Permeability MRI in a Rat Model of Transient Cerebral Ischemia

S.S. Ahn, S.H. Kim, J.E. Lee, K.J. Ahn, D.J. Kim, H.S. Choi, J. Kim, N.-Y. Shin and S.-K. Lee

AJNR Am J Neuroradiol 2015, 36 (2) 283-288
doi: https://doi.org/10.3174/ajnr.A4113
http://www.ajnr.org/content/36/2/283

Effects of Agmatine on Blood-Brain Barrier Stabilization Assessed by Permeability MRI in a Rat Model of Transient Cerebral Ischemia

S.S. Ahn, S.H. Kim, J.E. Lee, K.J. Ahn, D.J. Kim, H.S. Choi, J. Kim, N.-Y. Shin, and S.-K. Lee

EBM 2

ABSTRACT

BACKGROUND AND PURPOSE: BBB disruption after acute ischemic stroke and subsequent permeability increase may be enhanced by reperfusion. Agmatine has been reported to attenuate BBB disruption. Our aim was to evaluate the effects of agmatine on BBB stabilization in a rat model of transient cerebral ischemia by using permeability dynamic contrast-enhanced MR imaging at early stages and subsequently to demonstrate the feasibility of dynamic contrast-enhanced MR imaging for the investigation of new therapies.

MATERIALS AND METHODS: Thirty-four male Sprague-Dawley rats were subjected to transient MCA occlusion for 90 minutes. Immediately after reperfusion, agmatine (100 mg/kg) or normal saline was injected intraperitoneally into the agmatine-treated group ($n = 17$) or the control group, respectively. MR imaging was performed after reperfusion. For quantitative analysis, regions of interest were defined within the infarct area, and values for volume transfer constant, rate transfer coefficient, volume fraction of extravascular extracellular space, and volume fraction of blood plasma were obtained. Infarct volume, infarct growth, quantitative imaging parameters, and numbers of factor VIII–positive cells after immunohistochemical staining were compared between control and agmatine-treated groups.

RESULTS: Among the permeability parameters, volume transfer constant and volume fraction of extravascular extracellular space were significantly lower in the agmatine-treated group compared with the control group (0.05 ± 0.02 minutes^{-1} versus 0.08 ± 0.03 minute^{-1}, $P = .012$, for volume transfer constant and 0.12 ± 0.06 versus 0.22 ± 0.15, $P = .02$ for volume fraction of extravascular extracellular space). Other permeability parameters were not significantly different between the groups. The number of factor VIII–positive cells was less in the agmatine-treated group than in the control group (3-fold versus 4-fold, $P = .037$).

CONCLUSIONS: In ischemic stroke, agmatine protects the BBB, which can be monitored in vivo by quantification of permeability by using dynamic contrast-enhanced MR imaging. Therefore, dynamic contrast-enhanced MR imaging may serve as a potential imaging biomarker for assessing the BBB stabilization properties of pharmacologic agents.

ABBREVIATIONS: DCE = dynamic contrast-enhanced; K^{trans} = volume transfer constant

BBB disruption occurs within 1–2 hours after acute ischemic stroke by inflammatory cytokines and proteases.[1] Although thrombolysis has been increasingly used for the treatment of acute ischemic stroke, reperfusion after thrombolytic therapy has been reported to enhance BBB breakdown and, consequently, symptomatic hemorrhagic transformation, which is a fatal complication of ischemic stroke.[2,3] Therefore, evaluation of the therapeutic effect of a BBB blocking agent is important to improve treatment outcomes in patients with stroke. One can estimate the permeability properties of the BBB by using various techniques; however, many of these methods are invasive or suitable only for animal models.[4] Many studies have used MR imaging to measure BBB permeability to develop a feasible clinical technique for evaluating the integrity of the BBB and predicting hemorrhagic transformation in acute ischemic stroke.[5-7] Dynamic contrast-enhanced (DCE)-MR imaging by using contrast agents, an emerging MR imaging technique based on kinetic modeling of microvascular permeability, enables quantification of BBB breakdown.[8] A recent animal study reported that increased permeability measured by MR imaging correlates well with BBB disruption and hemorrhagic transformation on histology.[9]

A number of investigators have explored the use of neuroprotective drugs in animal experimental models to salvage regions of

Received April 28, 2014; accepted after revision July 31.

From the Department of Radiology and the Research Institute of Radiological Science (S.S.A., D.J.K., J.K., N.-Y.S., S.-K.L.), Department of Pathology (S.H.K.), Brain Research Institute, and Department of Anatomy (J.E.L.), Yonsei University College of Medicine, Seoul, Republic of Korea; and Department of Radiology (K.J.A., H.S.C.), The Catholic University College of Medicine, Seoul, Seoul, Republic of Korea.

Please address correspondence to Seung-Koo Lee, MD, PhD, Department of Radiology and the Research Institute of Radiological Science, Yonsei University College of Medicine, 50 Yonsei-ro, Seodaemun-gu, Seoul 120-752, Republic of Korea; e-mail: slee@yuhs.ac, lee.seungkoo@gmail.com

EBM 2 Evidence-Based Medicine Level 2.

http://dx.doi.org/10.3174/ajnr.A4113

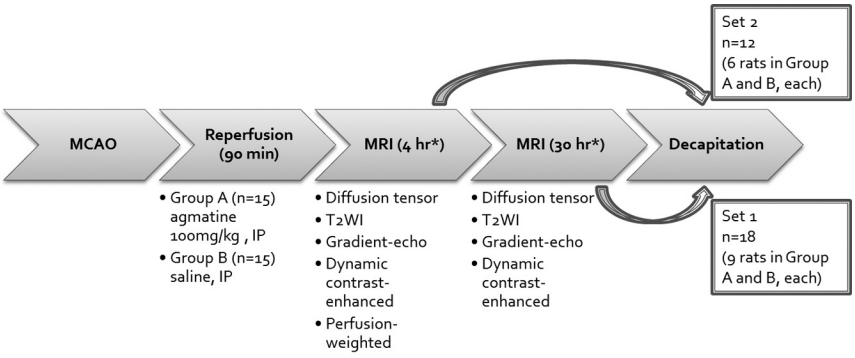

FIG 1. Flowchart overview of the experimental protocols.

ischemia and to minimize reperfusion injury.[10-12] Agmatine is a primary amine formed by decarboxylation of L-arginine and has been shown to protect neurons by blocking the *N*-methyl-*D*-aspartate receptor or nitric oxide synthase.[13] Because a previous animal study reported that agmatine showed a protective effect in rodent models of neurotoxic and ischemic brain injuries,[14] many additional studies have also shown beneficial effects of agmatine and its mechanisms.[15-17] Another recent study also suggested that agmatine attenuated BBB disruption and consequently reduced brain swelling when administered at the time of reperfusion.[11]

Therefore, the aim of this study was to quantitatively evaluate the BBB stabilization effect of agmatine in rat models of transient cerebral ischemia by using DCE-MR imaging at early stages and subsequently to demonstrate the feasibility of DCE-MR imaging for the investigation of new therapies.

MATERIALS AND METHODS

Animal Preparation

All animal procedures were performed according to a protocol approved by the Institutional Animal Care and Use Committee in accordance with National Institutes of Health guidelines. Thirty-four male Sprague-Dawley rats (Orient Bio, Seongnam, Korea) weighing 250–300 g were subjected to transient middle cerebral artery occlusion. Animals were anesthetized with Xylazine, 10 mg/kg, and Zoletil, a combination of tiletamine and zolazepam, 30 mg/kg, intraperitoneally. Rectal temperature was maintained at 37°C by a heating pad during the operation. The depth of anesthesia was assessed by toe pinch every 15 minutes. Middle cerebral artery occlusion was induced by using the filament model as previously described.[18] Briefly, under an operating microscope, an uncoated 23-mm segment of 4–0 polypropylene monofilament suture with the tip rounded by flame was inserted into the arteriotomy and advanced into the internal carotid artery approximately 19–20 mm from the bifurcation to occlude the ostium of the middle cerebral artery. After 90 minutes, the suture was withdrawn and surgical incisions were closed. The animal was allowed to awaken and recover with free access to food and water. We injected 100 mg/kg of agmatine mixed in normal saline solution intraperitoneally immediately after reperfusion in the agmatine-treated group ($n = 17$). In the experimental control group, the animals received an equivalent volume of normal saline ($n = 17$). The experimental design is shown in Fig 1. Four rats were excluded because they died before MR imaging acquisition (2 rats in the agmatine-treated group and 2 rats in the control group). Seven rats died after MR imaging acquisition and before we obtained pathologic specimens (2 rats in the agmatine-treated group and 5 rats in the control group), and they were included only for image analysis.

Image Acquisition

After anesthesia with Rumpun, 10 mg/kg, and Zoletil, 30 mg/kg, intraperitoneally, MR imaging was performed by using a 3T system (Achieva; Philips, Best, Netherlands) and an 8-channel coil. Animals were divided into 2 sets to correlate MR imaging with histopathology at 2 different stages. MR imaging was performed 4 and 30 hours after reperfusion in 18 rats (set 1: $n = 9$ agmatine-treated, $n = 9$ controls) and only 4 hours after reperfusion in 12 rats (set 2: $n = 6$ agmatine-treated, $n = 6$ controls) before obtaining the specimens. All images were obtained in the coronal plane with a 60-mm FOV. Pre- and postcontrast T1-weighted (TR/TE, 625/18 ms), T2-weighted (TR/TE, 2006/80 ms), and T2*-weighted (TR/TE, 549/16 ms) images were acquired with 2-mm section thickness, 0.2-mm section gap, and 192 × 192 matrix. Diffusion-tensor imaging was performed by applying 6 different directions of orthogonal diffusion gradients and b-values of 600 and 0 s/mm^2 (TR/TE, 3327/52 ms; 2-mm section thickness; 0.2-mm section gap; 128 × 128 matrix). To achieve quantitative hemodynamic measurements of cerebral permeability and perfusion, we injected 2 boluses via tail veins. The first bolus of contrast was administered to measure permeability and served as a preload bolus for the perfusion scans. For DCE-MR imaging, precontrast 3D T1-weighted images were obtained with the following parameters: TR/TE, 13.2/6.5 ms; 112 × 112 mm matrix; 2-mm section thickness; 0.2-mm section gap; and flip angle, 5°.

After the precontrast scan, 60 dynamic contrast-enhanced T1-weighted images were obtained with the same MR imaging parameters except for an increased flip angle of 15°. After acquisition of the fifth image volume, gadolinium-based contrast, gadobutrol (Gadavist, 0.2 mmol/kg; Bayer Schering Pharma, Berlin, Germany) was injected. The total scan time for DCE-MR imaging was 4 minutes 30 seconds with a temporal resolution of 4.5 seconds. Perfusion-weighted imaging (the rapid principles of echo shifting with a train of observations; TR/TE, 26.6/38.2 ms; 64 × 64 matrix) with 60 dynamic scans was performed following injection of the second bolus of Gadavist (0.2 mmol/kg) 4 hours after reperfusion. Relative cerebral blood volume maps were acquired by using commercially available postprocessing software (ViewForum; Philips), and reperfusion status was examined. All animals showed >90% relative cerebral blood volume of the contralateral hemisphere.

Image Analysis

Quantitative imaging analysis was performed by an investigator (a neuroradiologist with 4 years of experience) blinded to the treatments. First, DICOM data of diffusion-tensor imaging were transferred to a commercial software package (nordicICE;

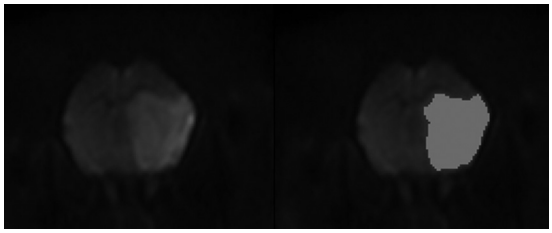

FIG 2. Semiautomatic measurement of infarct volume on diffusion-weighted imaging. The infarcted area with diffusion restriction is semiautomatically segmented (right) by using a commercial software package.

NordicNeuroLab, Bergen, Norway). On diffusion-weighted images, infarct volumes were calculated by using a semiautomated thresholding method to identify regions of interest with high signal intensity (Fig 2), and infarct volume fraction was expressed as a percentage of the ipsilateral hemisphere volume. Then, volumes of infarct growth were calculated in set 1.

All images were reviewed, and sections with the largest infarct area, near the sections of Bregma 1.60 mm, were selected for quantitative analysis of DCE-MR imaging.

All image data from DCE-MR imaging were transferred to an independent workstation for analysis. Permeability parameters for each pixel from DCE-MR imaging—volume transfer constant (K^{trans}), rate transfer coefficient, volume fraction of extravascular extracellular space, and volume fraction of blood plasma—were calculated, and color-coded parametric maps were generated by off-line Pride tools provided by Philips, which are based on the pharmacokinetic 2-compartment model of Tofts and Kermode.[8] Postprocessing was composed of motion correction of pixels from dynamic images, T1 mapping by using different flip angles (5° and 15°), registration of pixels on the T1 map, arterial input function estimation, and pharmacokinetic modeling. All these processes were automatically performed by Pride tools except drawing ROIs for the arterial input function. Arterial input function was measured several times at the area of the left internal carotid artery, and the proper arterial input function showing high amplitude, early sharp rise, and fast decay was selected for processing. Each permeability parameter was obtained in the infarct area. Permeability maps were also used for estimating brain tissue volume with BBB disruption, which was measured by obtaining pixel values and counting the numbers of pixels with K^{trans} of >0. Volume with BBB disruption was also expressed as a percentage of the ipsilateral hemisphere.

Pathologic Specimens

After performing MR imaging, the rats were anesthetized with Zoletil, 150 mg/kg, intravenously and perfused transcardially with 4% paraformaldehyde until the outflow fluid from the right atrium was colorless. The brain was rapidly removed and embedded in paraffin for histologic processing. Coronal sections (6-μm thick) were taken at 2-mm intervals through the brain region corresponding to the MR imaging sections and stained with hematoxylin-eosin for histopathologic evaluation. Gross hemorrhage was defined as blood evident to the unaided eye on the hematoxylin-eosin-stained sections and confirmed by microscopy. Microscopic hemorrhage was defined as blood evident only by microscopy (original magnification ×40).

Immunohistochemical Analysis

Seven rats were used in each group for immunohistochemical analysis. Paraffin-embedded sections were rehydrated. After permeabilization with proteinase K, sections were immunostained with primary antibodies against factor VIII (1:200 dilution) followed by biotinylated secondary antibodies. Sections were visualized by using horseradish peroxidase and then reacted with diaminobenzidine (DAB) as a substrate.

Images were observed and captured on an AX80 microscope equipped with a DP-72 digital camera (Olympus, Shinjuku, Tokyo, Japan). The stained cells were assessed in 2 consecutive coronal sections with the largest infarct areas from each rat. All data for immunohistochemistry were collected from 10 high-power fields (original magnification, ×200) within the infarct area per slide. These included 5 regions from the striatum, 3 regions from the parietal cortex, and 2 regions from the border area of infarct showing the highest expression. Another 10 regions were selected in the corresponding area in the contralateral hemisphere.

The captured images from immunohistochemistry were analyzed by an investigator blinded to the treatments with the aid of ImageJ software (National Institutes of Health, Bethesda, Maryland). The numbers of factor VIII–positive cells were counted in 10 images from the infarct area and contralateral hemisphere and expressed as a ratio.

Statistical Analysis

Infarct volume and volume with BBB disruption showed interaction with groups and time; therefore, linear mixed modeling followed by Bonferroni correction was used for between-group comparisons and within-group comparisons at different time points. Otherwise, independent *t* tests were performed to compare infarct growth, quantitative imaging parameters, and numbers of factor VIII–positive cells between control and agmatine-treated groups on the basis of normality testing by the Kolmogorov-Smirnov test. All statistical analyses were performed by using statistical software (SAS, Version 9.2 m; SAS Institute, Cary, North Carolina). *P* values < .05 were considered significant.

RESULTS

Image Analysis

To investigate the effect of agmatine on ischemic damage, we assessed infarct volume by MR imaging and found that agmatine significantly reduced infarct volume. Absolute infarct volumes were 160.7 ± 69.4 mm^3 in the agmatine-treated group and 250 ± 60.4 mm^3 in the control group at 4-hour reperfusion ($P < .001$). Infarct-volume fractions to the ipsilateral brain volume were 36.1 ± 10.8% in the agmatine-treated group and 54.2 ± 7.1% in the control group at 4-hour reperfusion ($P < .001$). At 30-hour reperfusion in set 1, infarct volumes were 45.8 ± 13% in the agmatine-treated group and 73.9 ± 10.8% in the control group ($P < .001$). In addition, infarct growth was less in the agmatine-treated group than in the control group (60 ± 44.4 mm^3 versus 130 ± 55.2 mm^3, $P = .009$).

DCE-MR imaging showed an increase in permeability parameters in the ipsilateral hemisphere of the middle cerebral artery occlusion. There were no cases with positive values of permeability parameters in the contralateral hemisphere on DCE-MR im-

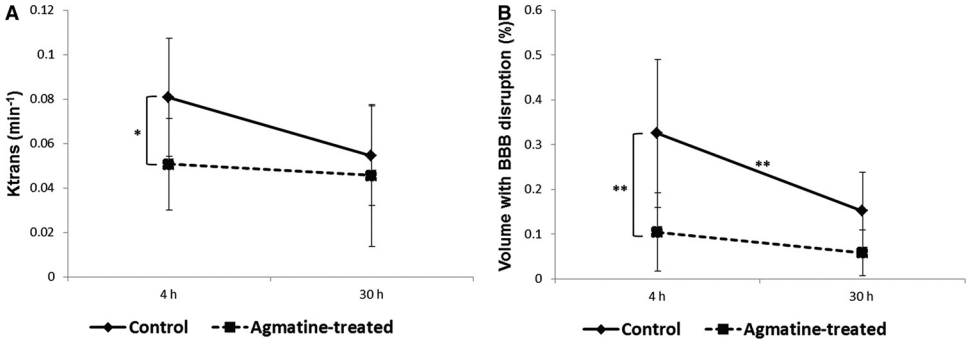

FIG 3. Permeability changes at 2 different time points. *A*, K^{trans} values. *B*, Brain tissue volume with BBB disruption expressed as a percentage of the ipsilateral hemisphere. *Square and diamond-shaped dots* are mean values; *horizontal lines* above and below the dots represent 95% confidence intervals. The *asterisk* indicates $P < .05$; 2 *asterisks*, $P < .01$).

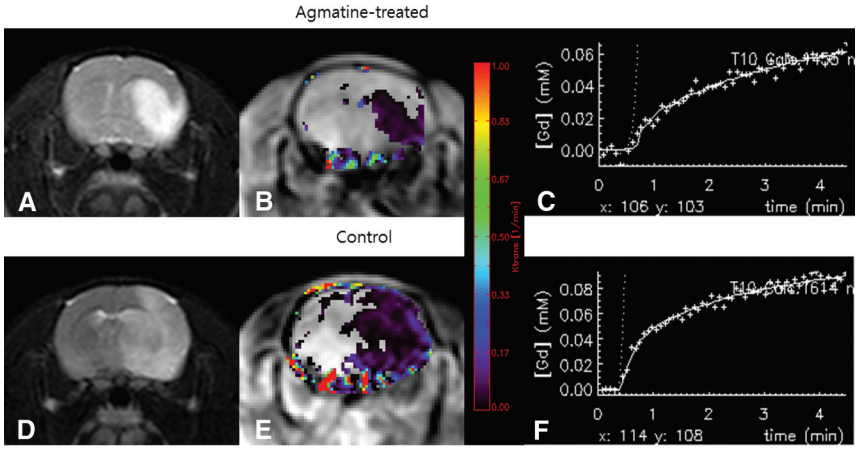

FIG 4. Representative MR images. Infarcted areas can be seen as hyperintensity on T2-weighted images (*A* and *D*). The color-coded permeability maps obtained 4 hours after reperfusion demonstrate increased permeability in the infarcted areas (*B* and *E*). The mean K^{trans} values were 0.05 ± 0.02 minutes^{-1} in the agmatine-treated groups and 0.08 ± 0.03 minutes^{-1} in the control group ($P = .012$). *C* and *F*, K^{trans} curves fit the data points (*small plus sign*) in the corresponding maps.

Permeability imaging parameters measured 4 hours after reperfusion[a]

	Control Group ($n = 15$)	Agmatine-Treated Group ($n = 15$)	*P* Value
K^{trans} (min^{-1})	0.08 ± 0.03	0.05 ± 0.02	.012
Kep (min^{-1})	0.46 ± 0.3	0.44 ± 0.28	.856
Ve	0.22 ± 0.15	0.12 ± 0.06	.02
Vp	0.042 ± 0.03	0.038 ± 0.02	.187
Volume of BBB disruption (%)	32.5 ± 16.5	10.4 ± 8.7	<.001

Note:—Kep indicates rate transfer coefficient; Ve, volume fraction of extravascular extracellular space; Vp, volume fraction of blood plasma.

[a] Data are means.

aging. Among the permeability parameters, K^{trans} and volume fraction of extravascular extracellular space were significantly lower in the agmatine-treated group compared with the control group (0.05 ± 0.02 minutes^{-1} versus 0.08 ± 0.03 minutes^{-1}, $P = .012$, for K^{trans} and 0.12 ± 0.06 versus 0.22 ± 0.15, $P = .02$, for volume fraction of extravascular extracellular space) 4 hours after reperfusion (Figs 3 and 4). However, K^{trans} and volume fraction of extravascular extracellular space measured 30 hours after reperfusion in set 1 were not significantly different between the 2 groups. Overall, there was a tendency of K^{trans} to decrease with time without statistical significance (0.06 ± 0.03 minutes^{-1} at 4-hour reperfusion versus 0.05 ± 0.03 minutes^{-1} at 30-hour reperfusion, $P = .06$). Other permeability parameters were not significantly different between the groups at each time point (Table). The volume with BBB disruption estimated from the permeability map was significantly less in the agmatine-treated group than in the control group. The volumes were $10.4 \pm 8.7\%$ in the agmatine-treated group and $32.5 \pm 16.5\%$ in the control group at 4-hour reperfusion ($P < .001$) (Fig 3). At 30-hour reperfusion in set 1, the volumes with BBB disruption were $5.8 \pm 5.1\%$ in the agmatine-treated group and $15.2 \pm 8.6\%$ in the control group ($P = .367$). Overall, the volume with BBB disruption at 30-hour reperfusion was significantly less than that at 4-hour reperfusion ($22.4 \pm 15.4\%$ at 4-hour reperfusion versus $10.5 \pm 8.4\%$ at 30-hour reperfusion, $P < .001$).

Histopathologic Analysis

On histopathologic examination, gross hemorrhage was observed within the ischemic region of 2 rats in the agmatine-treated group and 2 rats in the control group. In addition, microscopic hemorrhage was observed in 1 agmatine-treated rat and 2 control rats.

The ratio of the number of factor VIII–positive cells in the ipsilateral to that in contralateral hemispheres was lower in the agmatine-treated group than in the control group (3.1-fold versus 4-fold, $P = .037$) (Fig 5). The ratio of the number of factor VIII–positive cells in the ipsilateral to that in contralateral hemispheres in set 2, from which histopathology was obtained after the first MR imaging acquisition, was lower than that in set 1 (2.8-fold versus 3.9-fold, $P = .021$).

DISCUSSION

In this study, we found that agmatine protects the BBB in ischemic stroke and the BBB stabilization effect of agmatine can be monitored in vivo by quantification of permeability by using DCE-MR imaging. K^{trans}, volume fraction of extravascular extra-

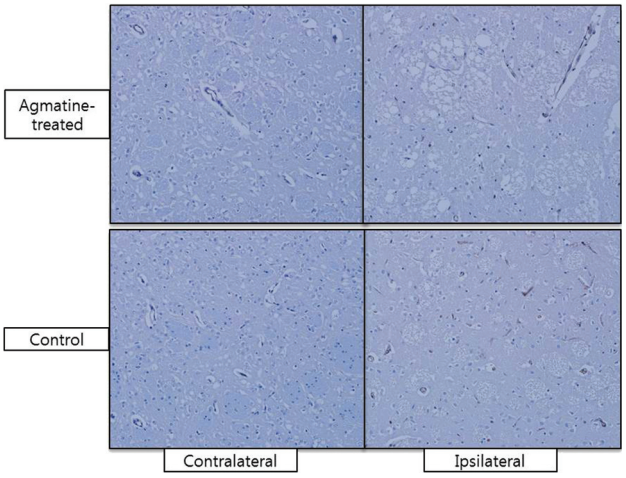

FIG 5. Immunohistochemical staining with primary antibodies against factor VIII. The ratio of the number of factor VIII–positive cells (brown) in the ipsilateral to that in contralateral hemisphere was lower in the agmatine-treated group (upper row) than in the control group (lower row) (3.1-fold versus 4-fold, $P = .037$) (original magnification ×200).

cellular space, and brain tissue volume with BBB disruption were significantly less in the agmatine-treated group than in the control group at 4-hour reperfusion. Our results support a previous study that showed the protective effects of agmatine on the BBB by using Evans blue.[11] Moreover, in another previous study, decreased expression of matrix metalloproteinase by agmatine was suggested as a possible mechanism limiting BBB disruption because matrix metalloproteinases are known to be associated with BBB disruption and subsequent vasogenic edema after cerebral ischemia.[19] Although Evans blue has been widely used to assess BBB disruption with its property of binding to serum albumin, it is only available for use in animal models.[20] DCE-MR imaging provides both permeability values and spatial maps of permeability changes without killing the animals, which enabled us to investigate the BBB blocking properties of pharmaceutical agents as a longitudinal study by acquiring multiple images at different time points. In addition, MR imaging is a more sensitive measure of BBB disruption because of the lower molecular weight of gadolinium compared with that of Evans blue as described in a previous experimental study (604.7 Da versus 75.8 kDa).[21] Therefore, in the present study, DCE-MR imaging was used for monitoring the time course of focal cerebral ischemia and the BBB stabilization effects of agmatine.

Our results showed a significant increase of K^{trans} and brain-tissue volume with BBB disruption at 4-hour reperfusion, which may be attributed to increased inflammatory and oxidative stress on the BBB after reperfusion.[20,22] There was a tendency of K^{trans} to decrease with time, and brain tissue volume with BBB disruption at 30-hour reperfusion was less than that at 4-hour reperfusion. Previous experimental studies have also shown a biphasic opening of the BBB after transient ischemic injury, which has been generally accepted.[20,23,24] Even though the mechanisms of this partial recovery of the BBB at 30-hour reperfusion are not well-understood, the results suggest that the reverse of reactive oxygen species-mediated disassembly of tight junction proteins within 6 hours may contribute to a decrease in the extravasation of gadolinium contrast agent.[23] On the other hand, recent animal studies have demonstrated continuous opening of the BBB.[21,25] However, they also observed a nonsignificant drop in gadolinium enhancement and Evans blue extravasation at 24- and 36-hour reperfusion, which can be explained by microvascular plugging caused by infiltrating neutrophils, fibrin, and platelets. Therefore, longitudinal studies with a large number of subjects need to be conducted to investigate temporal changes of the BBB and its mechanisms.

We performed immunohistochemical staining with factor VIII to assess angiogenesis following cerebral ischemia and found that the expression of factor VIII–positive cells was less in the agmatine-treated group than in the control group. These results may be because BBB disruption in the agmatine-treated group was significantly less than that of the control group according to DCE-MR imaging. Because the formation of new microvessels is a hallmark tissue response to ischemic injury, reduced expression of factor VIII–positive cells in the agmatine-treated group may be attributed to the protective effect of agmatine on the BBB. Overall, the expression of factor VIII–positive cells was lower at 4-hour reperfusion than at 30-hour reperfusion. Although expression of angiogenesis-related factors begins within 1–2 hours after focal ischemia, it increases for up to 14 days[1]; therefore, new vessels can be visualized better at later stages.

An increase in permeability measured by DCE-MR imaging may not directly reflect hemorrhagic transformation because the size of the gadolinium molecule is much smaller than that of red blood cells. Although BBB disruption was demonstrated in all cases of transient ischemic stroke, gross hemorrhage was observed in 2 rats of the agmatine-treated group and 2 rats of the control group. Therefore, on the basis of the results from this study, it is difficult to say whether agmatine would have a potential benefit preventing gross hemorrhage, which is clinically significant.

Agmatine was administered immediately after reperfusion because this timing is optimal for using agents with BBB blocking properties in a clinical setting. In addition, a previous animal experimental study reported that agmatine showed neuroprotective effects up to 4 hours after reperfusion.[16] Further studies are needed to investigate functional recovery and ultimate stroke outcome when agmatine is administered early, late, or throughout the phase of ischemic injury because timely pharmacotherapy is important for dynamic temporal changes in BBB permeability.

If the treatment window for effective reperfusion therapy can be expanded with agmatine, considerably more patients with stroke would be eligible for therapy. The results of the present study suggest that DCE-MR imaging has the potential to provide imaging biomarkers that are valuable for adjunctive therapy to reduce complications associated with thrombolytic therapy in ischemic stroke.

There are several limitations in our study. First, spatial maps of permeability could not be correlated with images of immunohistochemical staining because it is not technically possible to match regions on both MR imaging and histopathology. Second, the long-term effects of agmatine could not be assessed because the rats were sacrificed to obtain pathologic specimens right after we performed MR imaging. Further studies are warranted to deter-

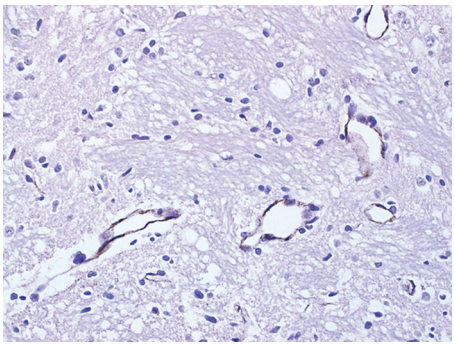

FIG 6. Immunohistochemical staining with high power (original magnification ×400). Factor VIII is stained in the endothelium along the blood vessels.

mine the neuroprotective effects of agmatine, such as functional recovery, with serial follow-up. Third, a 3T MR imaging scanner, which is not dedicated for animal imaging, was used in this study. However, it is commonly used in clinical practice, and acceptable images can be obtained to evaluate permeability in rat stroke models. Thus, a 3T MR imaging scanner with the methods identical to those used in this study may possibly be applied in humans. Last, because we had tried to stain the brain tissue by immunoperoxidase, we did not perform reference staining such as 4′,6-diamidino-2-phenylindole staining, which is necessary to prove that the factor VIII was stained in the cell. Instead, we confirmed that factor VIII was stained in the endothelium along the blood vessels with higher power magnification (original magnification ×400) (Fig 6).

CONCLUSIONS

Agmatine protects the BBB in ischemic stroke, which can be monitored in vivo by quantification of permeability by using DCE-MR imaging. Therefore, DCE-MR imaging may serve as a potential imaging biomarker for assessing the BBB stabilization properties of pharmacologic agents, including agmatine, at early stages to reduce complications associated with thrombolytic therapy in ischemic stroke.

ACKNOWLEDGMENTS

Special thanks to Ah-Reum Yang and Jae Young Kim (Department of Anatomy, Yonsei University College of Medicine, Seoul, Korea), who helped us through the experimental processes from making the animal experimental models to obtaining pathologic specimens. The authors are grateful to Sei Young Kim (MR imaging technician, Severance Hospital, Seoul, Korea) for his help with the examinations and for his valuable suggestions.

Disclosures: Dong Joon Kim—*UNRELATED*: *Grants/Grants Pending*: Yonsei University College of Medicine faculty grant, Korea Healthcare Technology R&D Project; *Patents (planned, pending or issued)*: stent delivery system.

REFERENCES

1. del Zoppo GJ, Mabuchi T. **Cerebral microvessel responses to focal ischemia.** *J Cereb Blood Flow Metab* 2003;23:879–94
2. **Tissue plasminogen activator for acute ischemic stroke: the National Institute of Neurological Disorders and Stroke rt-PA Stroke Study Group.** *N Engl J Med* 1995;333:1581–87
3. Berger C, Fiorelli M, Steiner T, et al. **Hemorrhagic transformation of ischemic brain tissue: asymptomatic or symptomatic?** *Stroke* 2001; 32:1330–35
4. Sood R, Taheri S, Estrada EY, et al. **Quantitative evaluation of the effect of propylene glycol on BBB permeability.** *J Magn Reson Imaging* 2007;25:39–47
5. Kassner A, Roberts T, Taylor K, et al. **Prediction of hemorrhage in acute ischemic stroke using permeability MR imaging.** *AJNR Am J Neuroradiol* 2005;26:2213–17
6. Bang OY, Buck BH, Saver JL, et al. **Prediction of hemorrhagic transformation after recanalization therapy using T2*-permeability magnetic resonance imaging.** *Ann Neurol* 2007;62:170–76
7. Wu S, Thornhill RE, Chen S, et al. **Relative recirculation: a fast, model-free surrogate for the measurement of blood-brain barrier permeability and the prediction of hemorrhagic transformation in acute ischemic stroke.** *Invest Radiol* 2009;44:662–68
8. Tofts PS, Kermode AG. **Measurement of the blood-brain barrier permeability and leakage space using dynamic MR imaging. 1. Fundamental concepts.** *Magn Reson Med* 1991;17:357–67
9. Hoffmann A, Bredno J, Wendland MF, et al. **Validation of in vivo magnetic resonance imaging blood-brain barrier permeability measurements by comparison with gold standard histology.** *Stroke* 2011;42:2054–60
10. Nonaka Y, Tsuruma K, Shimazawa M, et al. **Cilostazol protects against hemorrhagic transformation in mice transient focal cerebral ischemia-induced brain damage.** *Neurosci Lett* 2009;452:156–61
11. Kim JH, Lee YW, Park KA, et al. **Agmatine attenuates brain edema through reducing the expression of aquaporin-1 after cerebral ischemia.** *J Cerebr Blood Flow Metab* 2010;30:943–49
12. Wang CC, Chio CC, Chang CH, et al. **Beneficial effect of agmatine on brain apoptosis, astrogliosis, and edema after rat transient cerebral ischemia.** *BMC Pharmacol* 2010;10:11
13. Gilad GM, Gilad VH. **Accelerated functional recovery and neuroprotection by agmatine after spinal cord ischemia in rats.** *Neurosci Lett* 2000;296:97–100
14. Gilad GM, Salame K, Rabey JM, et al. **Agmatine treatment is neuroprotective in rodent brain injury models.** *Life Sci* 1996;58:PL 41–46
15. Feng Y, Piletz JE, Leblanc MH. **Agmatine suppresses nitric oxide production and attenuates hypoxic-ischemic brain injury in neonatal rats.** *Pediatric Res* 2002;52:606–11
16. Kim JH, Yenari MA, Giffard RG, et al. **Agmatine reduces infarct area in a mouse model of transient focal cerebral ischemia and protects cultured neurons from ischemia-like injury.** *Exp Neurol* 2004;189:122–30
17. Kim DJ, Kim DI, Lee SK, et al. **Protective effect of agmatine on a reperfusion model after transient cerebral ischemia: temporal evolution on perfusion MR imaging and histopathologic findings.** *AJNR Am J Neuroradiol* 2006;27:780–85
18. Longa EZ, Weinstein PR, Carlson S, et al. **Reversible middle cerebral artery occlusion without craniectomy in rats.** *Stroke* 1989;20:84–91
19. Kim JH, Lee YW, Kim JY, et al. **The effect of agmatine on expression of MMP2 and MMP9 in cerebral ischemia.** *Korean J Anatomy* 2008;41:97–104
20. Belayev L, Busto R, Zhao W, et al. **Quantitative evaluation of blood-brain barrier permeability following middle cerebral artery occlusion in rats.** *Brain Res* 1996;739:88–96
21. Strbian D, Durukan A, Pitkonen M, et al. **The blood-brain barrier is continuously open for several weeks following transient focal cerebral ischemia.** *Neuroscience* 2008;153:175–81
22. Heo JH, Han SW, Lee SK. **Free radicals as triggers of brain edema formation after stroke.** *Free Radic Biol Med* 2005;39:51–70
23. Pillai DR, Dittmar MS, Baldaranov D, et al. **Cerebral ischemia-reperfusion injury in rats: a 3 T MRI study on biphasic blood-brain barrier opening and the dynamics of edema formation.** *J Cereb Blood Flow Metab* 2009;29:1846–55
24. Kuroiwa T, Ting P, Martinez H, et al. **The biphasic opening of the blood-brain barrier to proteins following temporary middle cerebral artery occlusion.** *Acta Neuropathol* 1985;68:122–29
25. Durukan A, Marinkovic I, Strbian D, et al. **Post-ischemic blood-brain barrier leakage in rats: one-week follow-up by MRI.** *Brain Res* 2009;1280:158–65